Acta Crystallographica Section D
Biological Crystallography
ISSN 0907-4449

A methodology and an instrument for the temperature-controlled optimization of crystal growth

M. Budayova-Spano,[a]*‡ F. Dauvergne,[a] M. Audiffren,[b] T. Bactivelane[b] and S. Cusack[a]

[a]EMBL Grenoble-Outstation, 6 Rue Jules Horowitz, BP 156, CEDEX 9, Grenoble 38042, France, and [b]CRMCN–CNRS, Campus de Luminy, Case 913, CEDEX 9, Marseille 13288, France

‡ Present address: Unit of Virus Host Cell Interactions, UMR 5233 CNRS-UJF-EMBL, 6 Rue Jules Horowitz, BP 156, 38042 Grenoble, France.

Correspondence e-mail: spano@embl-grenoble.fr

Received 8 August 2006
Accepted 13 December 2006

A method and a device for the promotion of crystal growth by keeping the crystallization solution metastable during the growth process are described. This is achieved by controlled temperature variation of the crystallization solution using parameters determined *in situ* during the growth process. The technique finds application in the growth of large high-quality crystals for neutron crystallography. Thus, it has been applied to grow large crystals of several proteins of interest such as human γ-crystallin E, PA-IIL lectin from *Pseudomonas aeruginosa*, yeast inorganic pyrophosphatase, urate oxidase from *Aspergillus flavus* and human carbonic anhydrase II.

1. Introduction

Understanding how macromolecules function benefits enormously from knowledge of their structure at the atomic level. The fields of X-ray and neutron crystallography utilize the diffraction from crystals to determine the precise arrangement of atoms within the macromolecule. Whilst X-ray crystallography is by far the most frequently employed, the two crystallographic methods are complementary, reflecting the different physical nature of the interaction of either X-rays or neutrons with atoms. This is most evident upon consideration of the visibility of H atoms using the two techniques. X-ray structures at medium resolution do not contain any information on the positions of the H atoms within an enzyme active site, for example, whereas neutron structure determination at a similar resolution can reveal critical protons or hydrogen-bonding networks, thus providing novel insights into the enzyme catalytic mechanism. Both techniques are clearly dependent on the availability of suitable single crystals of good quality (*i.e.* low mosaicity, long-range order, strong diffraction, sufficient volume *etc.*) and obtaining these still remains an important bottleneck in biomacromolecular crystallography. Whilst the development of third-generation synchrotron sources has allowed X-ray protein structures to be solved from crystals of a few micrometres in their smallest dimensions, a major hurdle to neutron protein crystallography is that unusually voluminous crystals ($\sim$1 mm^3) are required to compensate for the weak flux of the available neutron sources (Myles *et al.*, 1998; Bon *et al.*, 1999; Coates *et al.*, 2001). However, if the protein is fully perdeuterated (all hydrogen replaced by deuterium) the required crystal volume can be considerably reduced. This is because perdeuteration significantly reduces the large incoherent scattering background of hydrogen and can thus provide a large gain in the signal-to-noise ratio of diffraction images (Gamble *et al.*, 1994; Shu *et al.*, 2000; Hazemann *et al.*, 2005). In addition, H–D exchange alters the physico-chemical properties of protein solutions and can affect the crystallization process in a significant way

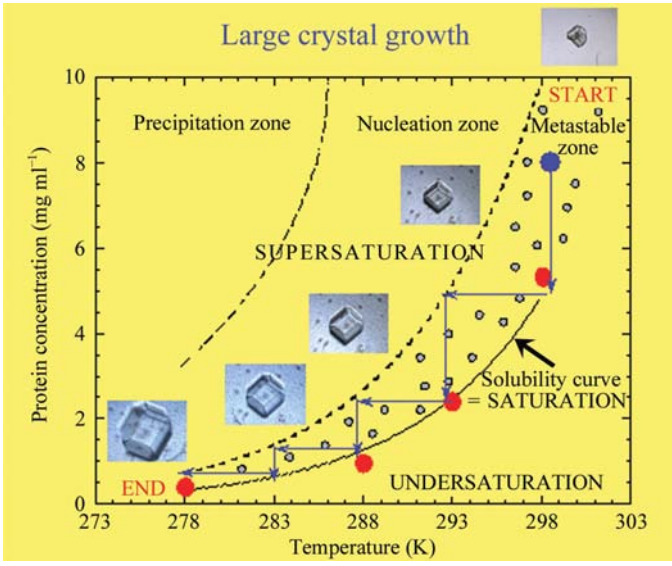

Figure 1
Phase diagram illustrating the control process for crystal growth in the metastable zone in the case of a protein with direct solubility. The solubility curve (red points) as well as the sequence representing the various steps (blue arrows) of the actual crystal-growth process of hydrogenated recombinant urate oxidase complexed with 8-azaxanthin in the presence of D_2O is schematized. The photographs show the crystal habits and volume of a seeded crystal observed before equilibration at 298, 293, 288, 283 and 278 K, respectively.

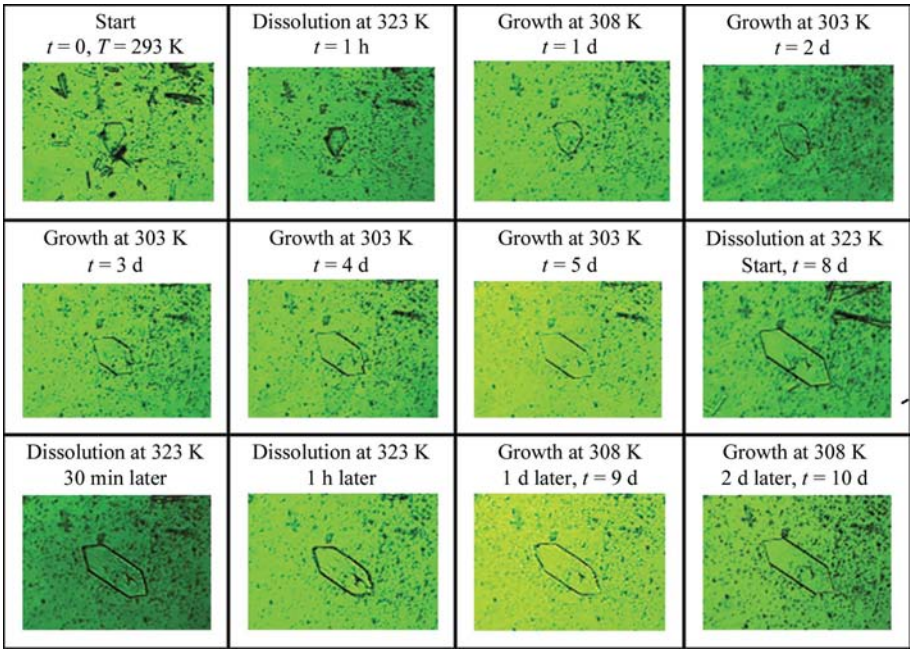

Figure 2
Determining the boundaries of the metastable domain in the case of perdeuterated human γ-crystallin E. Nucleation appears around the crystal of interest (seed illustrated in the centre of picture) at 293 K. During the first hour, partial dissolution of the seed crystal and total dissolution of the small nuclei surrounding it are observed at 323 K. Subsequently, the seed crystal grows during the next 5 d, firstly at 308 K and thereafter lowering the temperature to 303 K. Some new nuclei are formed at 303 K. Partial dissolution of the crystal occurs at 323 K during a subsequent hour in order to redissolve the new nuclei. Finally, the crystal is grown again at 308 K in order to increase its size and after 8 d no significant nucleation is observed.

(Gripon *et al.*, 1997; Budayova-Spano *et al.*, 2000). Indeed, understanding the solubility and phase behaviour of proteins is an essential part of the crystallization process. The growth of crystals from a protein solution requires the existence of a phase transition, which allows the protein state to be manipulated between at least two thermodynamic phases: soluble and crystalline. Crystal nucleation and growth arise on the boundary between these two phases and are governed by subtle effects in physical chemistry. Here, we describe a method and a device that allow the manipulation of the thermodynamics as well as the kinetics of the crystallization process, taking advantage of generic features of the phase diagram. The novelty in our approach is the combined use of temperature control and seeding to drive the process of the crystallization of biomacromolecules, both of which techniques individually represent powerful tools for the separation of nucleation and growth. We have constructed a device that enables the phase diagram to be investigated, the nucleation and crystal growth of biological macromolecules to be controlled and the solubility of seeded H/D-labelled biological macromolecule crystals to be manipulated *via* controlled temperature changes. Thus, the device allows the determination of the favourable zone of the phase diagram (metastable or growth phase) required for the optimized growth of crystals and can improve crystal volume and quality. The main part of this device is a custom-built multi-well temperature-controlled apparatus for crystallization. This assembly can be coupled to many types of inverted optical microscopes, thus combining *in situ* observation, image acquisition and processing with real-time and accurately controlled temperature variation. Furthermore, the crystals can be easily harvested from the device. We demonstrate here the effectiveness of both the method and the device with a panel of protein systems chosen for their research interest (Table 1) rather than typical model proteins.

2. Experimental methods

2.1. Crystallization protocols

The proteins used in this study, perdeuterated human carbonic anhydrase II (Budayova-Spano, Fisher *et al.*, 2006), perdeuterated yeast inorganic pyrophosphatase (Tuominen *et al.*, 2004), perdeuterated human γ-crystallin E (Artero *et al.*, 2005) and perdeuterated PA-IIL lectin from *Pseudomonas aeruginosa* (Mitchell *et al.*, 2002), were produced and purified following established protocols. Recombinant hydrogenated urate oxidase from *Aspergillus*

Table 1
Summary providing some physico-chemical properties and the crystal-growth conditions as well as the biological functions of the protein systems studied.

Protein system	MW (kDa)	pI classification	Crystallization conditions	*T* range (K)	Biological function
Hydrogenated urate oxidase from *A. flavus*	33.8	Basic, 7.5	Batch, 200 µl: ∼5% PEG 8000, 100 m*M* NaCl, 8 mg ml^{-1} protein, 50 m*M* Tris–HCl pD 8.5	278–298	Catalysis of the oxidation of uric acid to allantoin
Perdeuterated human γ-crystallin E	21	Basic, 7.2	Batch, 100 µl: 10% PEG 3350, 5 mg ml^{-1} protein, 200 m*M* magnesium acetate pD 7.4	278–323	Liquid–liquid phase separation in mammalian cataracts
Perdeuterated human carbonic anhydrase II	30	Acidic, 6.8	Batch, 100 µl: 1.15 *M* sodium citrate, 8 mg ml^{-1} protein, 100 m*M* Tris–DCl pD 7.5	278–313	Catalysis of the reversible hydration of carbon dioxide
Perdeuterated yeast inorganic pyrophosphatase	33.8	Acidic, 5.35	Batch, 200 µl: 15% MPD, 1 m*M* $MnCl_2$, 1 m*M* phosphate, 10 mg ml^{-1} protein, 30 m*M* MES pD 6.0	278–293	Phosphoryl-transfer reactions catalysed by multiple metal ions
Perdeuterated PA-IIL lectin from *P. aeruginosa*	12.5	Acidic, 3.9	Batch, 100 µl: 20% PEG 8000, 2 m*M* $CaCl_2$, 150 m*M* $(NH_4)_2SO_4$, 8 mg ml^{-1} protein, 100 m*M* Tris–HCl pD 8.2	278–313	Pathogen adhesion

flavus expressed in *Saccharomyces cerevisiae* (or rasburicase; EU trade name Fasturtec, USA trade name Elitek) was supplied and purified by Sanofi–Aventis. A purine-type inhibitor (8-azaxanthin) and the buffers, salts, PEGs and additives used in this study were purchased from Sigma–Aldrich. Prior to dissolution, the proper amounts of salts, PEGs, buffers and additives were dissolved in heavy water (Euriso-top, 99.92% D_2O) to obtain solutions with the concentrations required for crystallization (Table 1). The pD of the buffers was adjusted with NaOD (Euriso-top, 99% D) and DCl (Euriso-top, 99.8% D) according to the formula $pD = pH_{meas} + 0.3314n + 0.0766n^2$, where $n = \%D_2O$ (Lumry *et al.*, 1951). All the solutions were filtered through 0.22 µm Millipore filters. In all the crystal-growth experiments, initial crystallization mixtures were obtained using batch and/or dialysis techniques (Ducruix & Giegé, 1992). Before starting the experiment, crystallization mixtures were centrifuged and filtered to remove all solid particles (precipitate, dust or nuclei). Finally, some of the crystallization mixtures intended for large crystal-growth experiments were incubated under oil in order to prevent evaporation occurring at higher temperatures (Chayen *et al.*, 1990). Details of the biological function, physico-chemical properties and crystal-growth conditions of the proteins studied here are provided in Table 1.

2.2. Investigation of the phase diagram

The phase diagram was investigated by seeding a protein solution in previously established crystallization conditions (*e.g.* determined by conventional hanging-drop vapour diffusion, batch or dialysis button). The seeds were observed through a microscope while the temperature was adjusted to slightly above or below the initial temperature. Upon temperature change, the following alternative events can be observed.

(i) The seeds grow and no spontaneous nucleation is observed. This corresponds to the metastable zone, where the supersaturation level is too low for nucleation, so that no new crystals form in any reasonable amount of time (Fig. 1).

(ii) The seeds dissolve. This corresponds to the zone of undersaturation (bottom right in Fig. 1). In order to detect the undersaturation/metastable boundary, the temperature should be varied to increase the supersaturation until the dissolution of seeds is stopped and saturation and crystal growth are attained.

(iii) The seeds grow and further nuclei form in the crystallization solution. This corresponds to the zone of spontaneous nucleation, where the supersaturation is large enough that spontaneous nucleation is observable (Fig. 1). In order to detect the nucleation/metastable boundary, the temperature should be varied to decrease the supersaturation until the formation of new nuclei is stopped and the growth of seeds is maintained.

(iv) Disordered structures such as aggregates or precipitates form which may prevent the growth of seeded crystallites as well as the formation of new nuclei. This corresponds to the precipitation zone, where the supersaturation is so large that aggregates and precipitates form faster than crystals (top left in Fig. 1).

For all the protein systems studied here (Table 1), we could demonstrate the reversibility of the formation of these precipitates by their dissolution after decreasing the supersaturation level using temperature as a variable under the studied crystallization conditions. All these zones are illustrated schematically for the case of direct protein solubility (protein solubility increases with temperature) in Fig. 1. Even though the division into zones is qualitative, the different behaviours serve as a guide when searching for the appropriate conditions to produce and grow crystals. During this process, the *in situ* observations need to be carried out regularly and at intervals of time of between a few seconds and several days. For example, protein denaturation and crystal dissolution as well as the formation of aggregates (precipitates) or new nuclei could be observed immediately or quickly,

typically in a few seconds to a few tens of minutes. In contrast, the time scale needed to observe crystal growth typically ranges from a few minutes to a few hours. When the equilibrium state between the crystal and the solution is approached, no significant difference in crystal size is observed over a few days. Fig. 2 and Supplementary Movie 1[1] show a series of photographs taken to detect the boundaries of the metastable zone in the case of perdeuterated human γ-crystallin E in the temperature range 303–323 K. On the other hand, Fig. 1 illustrates the crystal growth of hydrogenated recombinant urate oxidase complexed with 8-azaxanthin in a more conventional temperature range (278–298 K).

2.3. Solubility measurements

Since the three zones inside the supersaturation region are related to kinetic phenomena, the boundaries between these zones are less well defined than the solubility curve, which is unambiguously defined as the equilibrium between the solution and the crystal. Since the crystal–solution equilibrium is significantly altered by H–D exchange (Gripon *et al.*, 1997; Budayova-Spano *et al.*, 2000), it is helpful to separately measure the protein-solubility curve under deuterated crystallization conditions before attempting crystal growth. The determination of the solubility curve is carried out by direct measurement of the protein concentration at the crystal–solution equilibrium at a given temperature (Ducruix & Riès-Kautt, 1990; Cacioppo *et al.*, 1991; Rosenberger *et al.*, 1993; Sazaki *et al.*, 1996; Haire & Blow, 2001). This is performed by seeding a supersaturated or undersaturated protein solution with crushed microcrystals. As the seeded crystals grow or dissolve, the protein concentration is monitored and determined regularly by removing aliquots and measuring the absorbance by spectrophotometry at 280 nm. When the concentration of the solution reaches a constant value, the system has reached equilibrium (Fig. 3) and the final protein concentration in solution corresponds to the solubility. It typically takes between a couple of days and about a week (depending on the volume of the seeding solution) to measure a point on the solubility curve. An example of a solubility curve measured as a function of temperature in the case of hydrogenated recombinant urate oxidase complexed with 8-azaxanthin in the presence of D_2O is shown in Fig. 1. In order to demonstrate the effects of D_2O on the equilibrium between the solution and the crystal, the urate oxidase solubility measured at different temperatures in D_2O was compared with values measured in H_2O (Fig. 4*a*). As observed previously (Gripon *et al.*, 1997; Budayova-Spano *et al.*, 2000), we find that the solubility of urate oxidase in D_2O is significantly lower than that in H_2O, corresponding to a shift of approximately 7.2 K (Fig. 4*b*).

2.4. Crystal-growth process

The principle of the method for promoting crystal growth is schematized in Fig. 1. The crystallization solution is seeded with protein crystals at some point in the metastable zone or on the solubility curve. Crystals (usually 5–50 µm in size) for macroseeding can be nucleated in the apparatus or by any other technique, *e.g. via* the hanging-drop method. By using only one seed, the size of the seed increases during growth and the result is a single large crystal. The crystal growth of the seeds is maintained inside the metastable zone for as long as possible with the aid of temperature variations just after the crystal–solution equilibrium is achieved (shown by arrows representing changes in temperature in Fig. 1). An example of the crystal-growth process is illustrated for hydrogenated recombinant urate oxidase complexed with 8-azaxanthin (Fig. 1) in the presence of D_2O. The growth process for a protein crystal starts at a temperature where the protein crystal is still thermally stable (*e.g.* at 298 K). In the first step, the growth temperature is initially kept stable, typically for a week. In fact, the time depends on the volume of crystallization solution. If lower crystallization volumes are used, shorter times are required. The process of crystal growth stops at a certain point, defined as the point at which the size of the crystal does not change any further owing to equilibrium between the protein solution and crystal (this is shown by the end of the first vertical arrow at the metastable/undersaturation boundary in Fig. 1). This is determined by taking photographs of the crystal approximately every 20–30 min when crystal growth is starting and every 2–3 h when crystal growth is ending and comparing the size of the crystal using image-processing software. The temperature is then adjusted in a second step to a temperature value that is estimated to be still within the metastable zone, *e.g.* 293 K, and growth of the crystal restarts. The rate of change of temperature is typically 5 K h^{-1}. The temperature is then held constant until equilibrium conditions are re-established and the crystal grows to a new size. The process corresponding to the equilibration step at 293 K (after 2 d growth) is shown in Supplementary Movie 2[1]. These steps are repeated until crystals with a size of about 1 mm, suitable for neutron crystallography, are obtained. To obtain crystals with this size may take as long as two months

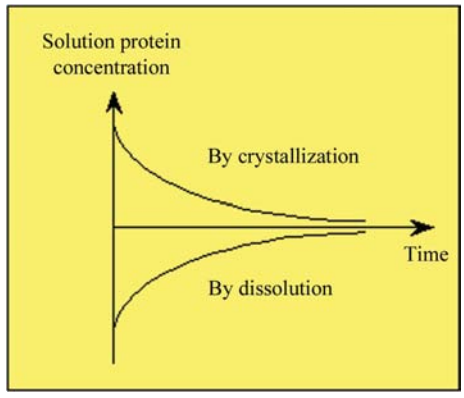

Figure 3
Schematic diagram illustrating the principle of solubility measurements.

[1] Supplementary material has been deposited in the IUCr electronic archive (Reference: FW5105). Services for accessing this material are given at the back of the journal.

because of the large crystallization volumes required. The temperature chosen for crystal growth depends on the type of protein used, as different proteins are less stable or denature above different specific temperatures. The optimal ranges of the temperature for the different protein systems studied here are summarized in Table 1.

2.5. Description of the apparatus

A complete semi-automated protein crystal-growth system for investigation of the phase diagram and controlled crystal growth is shown in Supplementary Fig. 1. It includes an inverted Leica DM IRB HC microscope, a Leica DFC 280 digital video camera, a computer (Intel Pentium 4 2.6 GHz processor, 512 MB RAM) and a PID (proportional–integral–derivative) electronic temperature controller and a crystal-growth apparatus produced in-house. The crystal-growth apparatus, which is incorporated onto the stage of the microscope, is shown disassembled in Fig. 5(*a*) and assembled in Fig. 5(*b*). The crystallization solution (25–1000 µl) is poured into a specially designed quartz cell with an optical bottom covered with a quartz air-tight cap, which is attached to a brass support incorporating a single well or several wells. The apparatus with several wells has a versatile circular carousel with a diameter of 8 cm equipped with 48 25 µl tubes (or six 1 ml tubes) maintained at the same temperature. The rotation and translation of the carousel are motorized (Fig. 5*a*). The accessible temperature range is from 233 to 353 K, with the temperature controlled by Peltier elements to an accuracy of 0.1 K. The cooling system of the Peltier elements helps to improve temperature regulation (Fig. 5*b*). In order to prevent condensation, particularly at low temperatures, a circuit of dry air is included (Fig. 5*a*). The microscope adaptor (Fig. 5) allows the crystal-growth apparatus to be mounted onto the microscope table in such a way that by rotating the carousel, the digital video camera of the microscope can view the different wells. The computer is equipped with the software program *Leica IM*500, which allows visualization and measurement of crystals, image acquisition, processing and storage. The temperature is controlled by a program developed in-house and written with *Labview*, which allows step-by-step, gradient or custom temperature variation. The temperature controller, as well as the corresponding software, was conceived to simultaneously control two crystal-growth experiments (*i.e.* with two crystal-growth apparatuses). In this way, one can work simultaneously at two different temperatures, for example. To facilitate the extraction of protein crystals after growth without causing any mechanical damage to the protein crystal, a micromanipulator (Model Eppendorf TransferMan NK2) has been added to the apparatus (Supplementary Fig. 1). The pivoting arm of the micromanipulator holds the quartz capillary to be used for harvesting the crystal and is attached to the table of the microscope. The tubing system was adapted to permit manipulation of the protein crystals. It includes a plastic syringe, a tube and a metallic spring. The main part of the micromanipulator, the digital box with joystick, enables the quartz capillary to be displaced inside the quartz cell containing the crystallization solution and the crystals with a precision of about 40 nm along each of the three axes. A light guide is added to improve the visualization of the top surface of the quartz capillary on the computer screen during the process of positioning and harvesting the crystals. Micromanipulation (removal and addition) of perdeuterated PA-IIL lectin crystals as well as positioning the top of the capillary in the crystallization solution are shown in Supplementary Movies 3, 4 and 5, respectively.

3. Results

As found previously (Budayova-Spano, Bonneté *et al.*, 2006), the crystals of hydrogenated recombinant urate oxidase

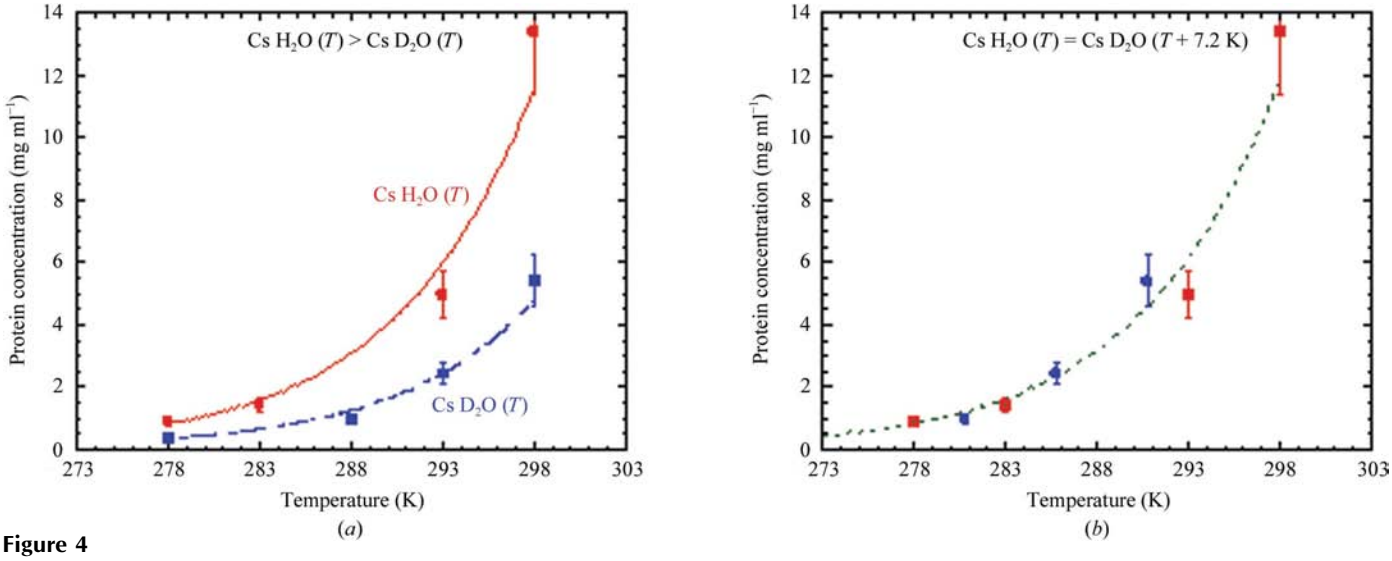

Figure 4
Temperature-dependence of the solubility of hydrogenated recombinant urate oxidase complexed with 8-azaxanthin in light and heavy water. (*a*) The solubility in D_2O is significantly lower than in H_2O and is shifted by approximately 7.2 K relative to that in H_2O (*b*). Error bars represent the maximum difference between the concentrations measured by absorption at 280 nm.

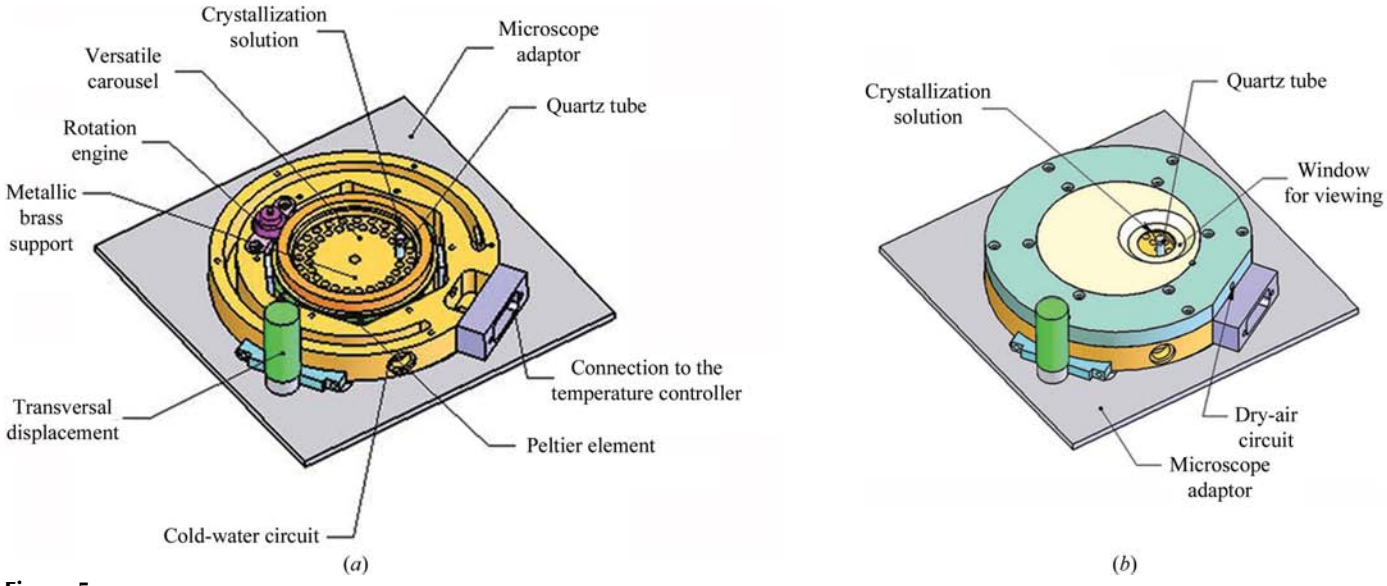

Figure 5
Crystal-growth apparatus: (*a*) disassembled position, (*b*) assembled position.

complexed with 8-azaxanthin provided by Sanofi–Synthélabo were multiple and thus unsuitable for structural analysis. However, large single crystals grown by careful control and optimization of crystallization conditions *via* knowledge of the phase diagram using the method and device described in this paper (Figs. 1 and 4) yielded high-quality neutron diffraction data (Budayova-Spano, Bonneté *et al.*, 2006), which were collected on the LADI instrument at the Institut Laue Langevin (ILL; Cipriani *et al.*, 1996). Fig. 6 shows a typical neutron Laue diffraction pattern obtained from a crystal with a volume of 1.8 mm^3, which diffracted to 2.1 Å resolution.

A further example of improved large crystal growth for neutron crystallography is provided by perdeuterated yeast inorganic pyrophosphatase (Fig. 7). In this case, working in the temperature range between 278 and 293 K allowed the stabilization and growth of the crystalline form of interest and avoided the growth of an alternative crystal form that can occur under the same crystallization conditions. The quality of the crystal grown by this method, as assessed by optical microscopy, appears to be better than the quality of the seed (which remains at the centre of the crystal). Preliminary neutron diffraction data have been collected on LADI (Cipriani *et al.*, 1996) from a crystal with a volume of 0.7 mm^3 and diffraction to better than 3.0 Å resolution was observed (unpublished results).

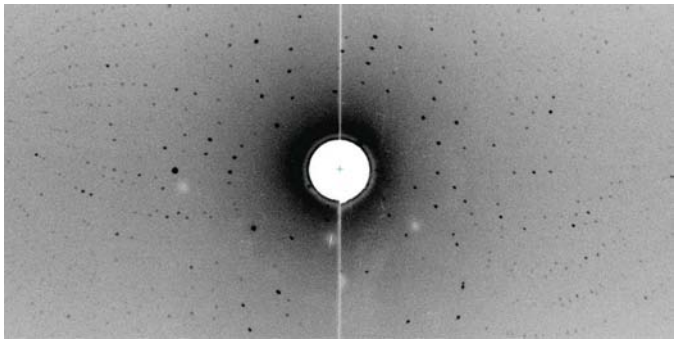

Figure 6
Typical neutron Laue diffraction pattern collected on LADI (ILL) from a 1.8 mm^3 crystal of recombinant urate oxidase complexed with 8-azaxanthin, which diffracted to 2.1 Å resolution.

Finally, improved large crystals obtained in the case of perdeuterated human carbonic anhydrase II proved to be useful for X-ray crystallography (Fig. 8). Initially, crystals of perdeuterated human carbonic anhydrase II were grown using the hanging-drop vapour-diffusion technique with 5 µl perdeuterated protein (20–30 mg ml^{-1}) mixed with 5 µl precipitant solution (100 m*M* Tris–DCl pD 7.5, 1.15 *M* sodium citrate) at 277 K (Budayova-Spano, Fisher *et al.*, 2006). Unfortunately, compared with hydrogenated protein, which gives large single crystals diffracting X-rays to 1.05 Å resolution (Fisher *et al.*, 2007), all crystals of perdeuterated protein obtained by traditional crystallization techniques under the same crystallization conditions produced clusters of poor crystal quality, diffracting to no better than 2.5 Å resolution (see Fig. 8*a*). However, crystal size and quality could be significantly improved using the methods and device describing in this paper (Figs. 8*b*, 8*c* and 8*d*). Finally, single crystals of perdeuterated human carbonic anhydrase II were obtained that diffracted X-rays to 1.5 Å resolution and were isomorphous to the hydrogenated form of the protein (Budayova-Spano, Fisher *et al.*, 2006). This example demonstrates the utility of this device to transform clusters of crystals into single crystals suitable for X-ray analysis.

4. Discussion

Whilst the X-ray structures of perdeuterated and hydrogenated proteins are essentially indistinguishable at near-atomic resolution (Artero *et al.*, 2005; Budayova-Spano, Fisher *et al.*, 2006), subtle differences in the physico-chemical properties of D_2O and H_2O affect protein–solvent and

protein–protein interactions and hence protein solubility in a significant way. For instance, it has been suggested that stronger attractive protein–protein interactions in D_2O (Gripon *et al.*, 1997; Budayova-Spano *et al.*, 2000) result from an enhanced hydrophobic effect in heavy water compared with light water (Kresheck *et al.*, 1965; Bonneté *et al.*, 1994). This suggests that the growth of large macromolecular crystals suitable for neutron diffraction analysis should benefit from a systematic study of the phase diagram under deuterated crystallization conditions. For instance, it has been found that lysozyme, BPTI and α-amylase have a lower solubility in D_2O than in H_2O and our solubility measurements with hydrogenated recombinant urate oxidase complexed with 8-azaxanthin show the same tendency (Fig. 4). The solubility of a macromolecule is a well defined thermodynamic concept: at any concentration of the crystallizing agent, a corresponding concentration of macromolecule is in equilibrium with the solid phase. In principle, any thermodynamic pathway leading from undersaturation to supersaturation should lead to crystallization (Ducruix & Giegé, 1992). Supersaturation is the driving force for the nucleation and growth process (Boistelle & Astier, 1988). However, thermodynamics only indicate that a process is energetically favourable; they say nothing about how quickly successive or competing processes will take place. Thus, efforts to control crystallization must be guided by an understanding of the thermodynamics as well as the kinetics of this non-equilibrium process. There are a variety of schemes that manipulate the kinetics of the crystallization process and all take advantage of generic features of these phase diagrams (Chayen & Saridakis, 2002; Luft & DeTitta, 1997).

Phase-diagram analysis and more active control of crystallization at the macroscopic level have been used previously to obtain crystals suitable for neutron diffraction experiments (Arai *et al.*, 2002; Maeda *et al.*, 2004; Niimura *et al.*, 2006). These authors have developed an apparatus based on a novel dialysis method allowing investigation of the two-dimensional phase diagram representing the protein *versus* precipitant concentration (Niimura *et al.*, 2006). In this device, the protein solution is separated from the precipitant solution by a dialysis membrane. The protein volume is then systematically varied and controlled by a syringe. The advantage of this technique is that any combination of protein and precipitant concentrations can be surveyed in a systematic manner and the total quantity of protein remains constant during the entire process of phase-diagram investigation. The disadvantage is that as the concentration of precipitant varies the technique requires the exchange of the crystallization solution in the reservoir.

In comparison, the main advantage of the method described here is that the protein volume and concentration as well as the precipitant volume and concentration remain constant during the entire process of phase-diagram investigation and crystal growth. The only variable in our system is the temperature, which is often ignored as an optimization variable and/or is poorly controlled. The novelty in our scheme is the combined use of the temperature control and seeding to drive the process of the crystallization of biomacromolecules, techniques which both individually represent powerful tools for the separation of nucleation and growth. Seeding is a powerful tool for controlled crystal growth, in which previously nucleated crystals are introduced into a crystallization solution equilibrated at lower levels of supersaturation, thus favouring slow ordered growth of large crystals. Seeding has been critical for obtaining diffraction-quality crystals for many structures (Bergfors, 2003). On the other hand, there are several reasons to choose temperature as a crystallization parameter. Temperature is an important variable in biological macromolecule and small-molecule crystallization (Boistelle & Astier, 1988; Ducruix & Giegé, 1992; Lorber & Giegé, 1992; Christopher *et al.*, 1998). Temperature change can provide precise, quick and reversible control of the relative supersaturation levels of crystalline solutions. Temperature control is non-invasive and can be used to manipulate sample solubility and crystallization without altering reagent formulation. Temperature governs the balance between enthalpy and entropy effects on free energy, which are typically comparable in magnitude. Depending on whether crystallization is enthalpy-driven or entropy-driven, proteins may become

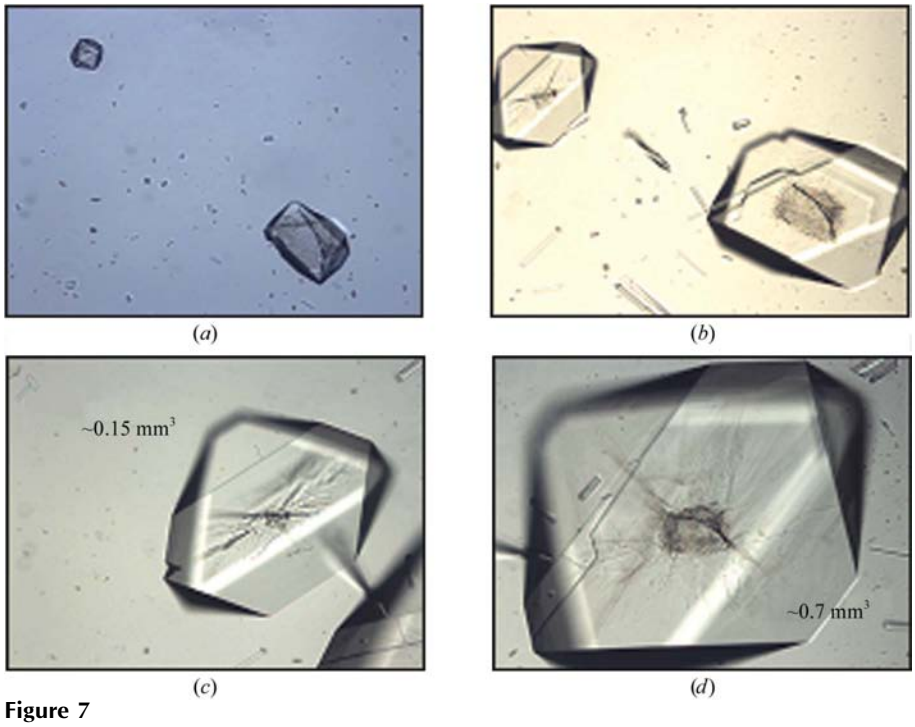

Figure 7
Improved large crystal growth for the neutron diffraction study of perdeuterated yeast inorganic pyrophosphatase. The photographs show the crystal habit and volumes of two seeded crystals at 293 K (*a*) and their crystal growth observed at 278 K one month (*b*) and two months later (*c*, *d*), respectively.

either more soluble at higher temperatures (direct solubility) or less soluble at higher temperatures (reverse solubility). Temperature influences nucleation and crystal growth by affecting the solubility and supersaturation of the sample and so can be used to carefully manipulate crystal nucleation and crystal growth. Temperature can affect different phases and growth mechanisms and then induce solution-mediated phase transitions (Boistelle & Astier, 1988; Lorber & Giegé, 1992; Budayova, 1998; Veesler *et al.*, 2003). On the other hand, temperature also affects the quantity, size and quality of the crystals. It can be used to dissolve smaller crystals for the benefit of larger ones. By analogy with what is known from the small-molecule field, the Ostwald ripening mechanism was proposed to account for this phenomenon (Boistelle & Astier, 1988; Ng *et al.*, 1996). In contrast to phase transitions, it concerns only crystals of the same composition and structure, *i.e.* crystals of the same phase. Fig. 2 and Supplementary Movie 1 illustrate one example of Ostwald ripening induced by temperature fluctuations in the case of perdeuterated human γ-crystallin E. Finally, temperature can also be used to etch or partially dissolve and then grow back the crystal in an attempt to improve the crystal volume and quality as demonstrated for the neutron diffraction experiments with hydrogenated recombinant urate oxidase complexed with 8-azaxanthin (Figs. 1 and 6) and with perdeuterated yeast inorganic pyrophosphatase (Fig. 7).

The case of perdeuterated human carbonic anhydrase II (Fig. 8) suggests that our technique can in certain circumstances be of use in optimization of crystal growth even for X-ray diffraction experiments. Indeed, when larger crystals of equally high quality are grown they provide certain advantages for X-ray diffraction. They are easier to handle, diffract more strongly and can be useful in overcoming the problem of radiation damage, since fresh volumes in the same crystal can consecutively be exposed. Another source of interest in the growth of large single crystals for X-ray crystallography is the fact that the size of the macromolecules under study has increased steadily over recent years and crystals of large assemblies are more frequently obtained but have weaker diffracting power owing to their larger unit-cell size and high solvent content. Finally, although high-throughput crystallization methods can produce initial crystallization conditions in many cases, the most interesting macromolecules can be challenging to crystallize into suitable single crystals owing to twinning or other crystal defect problems. Another suggestion is to test this technique in the future for protein systems that are very difficult to crystallize, such as membrane proteins. Temperature has been shown to be an important parameter in the phase behaviour of detergent solutions as well as detergent–monoolein mixtures during membrane-protein crystallization (Garavito & Picot, 1991; Sennoga *et al.*, 2003). Finally, our proposed technique also offers interesting possibilities for small-molecule crystallization in the pharmaceutical industry, where the avoidance of polymorphism can become critical. Temperature has been shown to be an efficient variable to favour obtaining a given polymorph (Veesler *et al.*, 2003).

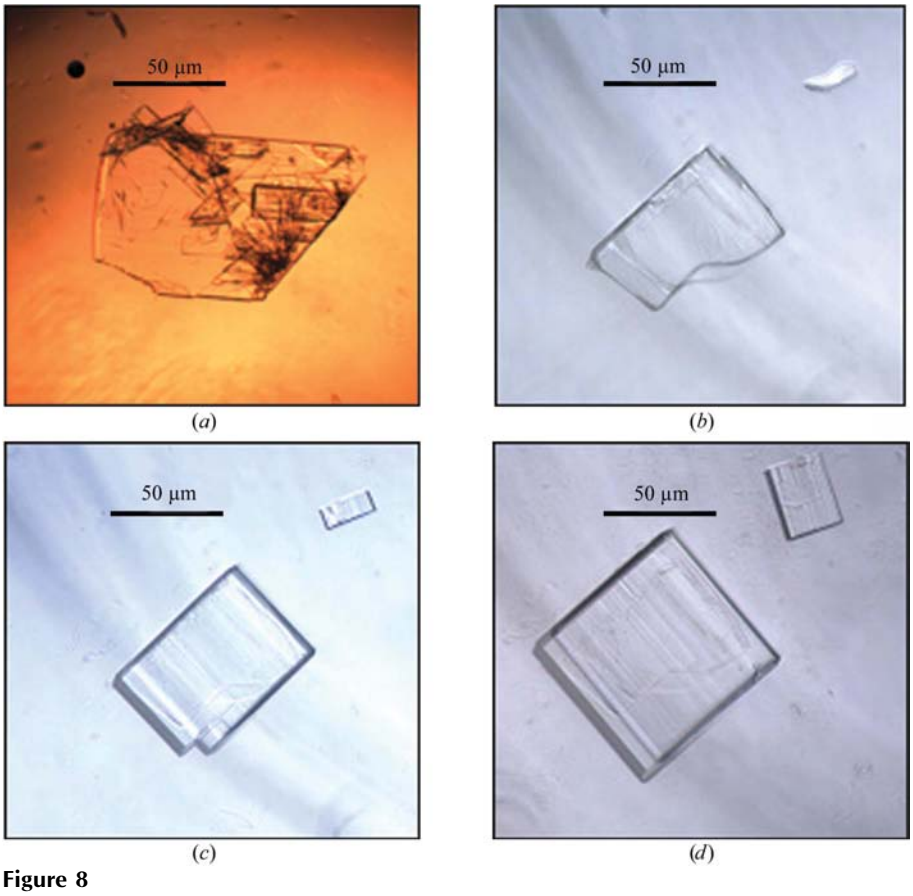

Figure 8
Improved large crystal growth for the X-ray diffraction study of perdeuterated human carbonic anhydrase II. The photographs show the crystal habit and size of a crystal cluster grown by the hanging-drop vapour-diffusion crystallization technique at 293 K (*a*) and of a seeded small piece of this crystal cluster at 308 K (*b*). Crystal growth of the seed observed after 3 d at 308 K (*c*) and after 6 d at 303 K (*d*) are also shown.

5. Conclusions

Here, we propose a novel method and apparatus that finds application in the growth of large high-quality crystals for neutron crystallography. It allows the manipulation of the thermodynamics as well as the kinetics of the crystallization process, taking advantage of generic features of the phase diagram. Knowledge of the phase diagram and the ability to control the temperature to drive the process of the crystallization of biomacromolecules allow us to tailor crystallization experiments to search for conditions that lead to crystals of a desired crystalline form, quality and size. The promotion of crystal growth is obtained by keeping the crystallization

solution metastable during the process of crystal growth. This is achieved by regulating the temperature of the crystallization solution using control parameters determined *in situ* during the growth process. The technique has been used to grow large crystals for neutron diffraction experiments of several proteins of interest (Table 1). The present work provides additional evidence that the crystallization of biological macromolecules proceeds by mechanisms similar to those involved in the crystallization of small molecules (Boistelle & Astier, 1988; Ducruix & Giegé, 1992; Bergfors, 2003; Chernov, 2003; Garcia-Ruiz, 2003; McPherson *et al.*, 2003; Asherie, 2004). From a practical point of view, we propose here an alternative and efficient way to obtain large high-quality biological macromolecular crystals. In addition, this work contributes to the development of automated crystal-growth optimization methods that should help to remove the main bottleneck in the application of neutron crystallography to structural biology.

The authors thank the staff of the ILL/EMBL Deuteration Laboratory in Grenoble, especially Marie-Thérèse Dauvergne, Dr Jean-Baptiste Artero and Dr Michael Haertlein, for providing the perdeuterated material and Professor Bertrand Castro and Dr Mohamed El Hajji of Sanofi–Aventis (Montpellier, France) for supplying the pure hydrogenated recombinant urate oxidase. We are grateful to Dr Stéphane Veesler, Jean-Pierre Astier (CRMCN–CNRS Marseille) and Dr William Shepard (Synchrotron Soleil, Saclay) for helpful conversations and insights. We extend special thanks to Dr Peter Timmins (ILL Grenoble) and Dr Dean Myles (Oak Ridge National Laboratory, USA), who took an active interest in taking forward the protein crystallization problem for neutron crystallography. We acknowledge support from the EU under the DLAB contracts HPRI-CT-2001-50035 and RII3-CT-2003-505925.

References

Arai, S., Chatake, T., Minezaki, Y. & Niimura, N. (2002). *Acta Cryst.* D**58**, 151–153.
Artero, J.-B., Härtlein, M., McSweeney, S. & Timmins, P. (2005). *Acta Cryst.* D**61**, 1541–1549.
Asherie, N. (2004). *Methods*, **34**, 266–272.
Bergfors, T. (2003). *J. Struct. Biol.* **142**, 66–76.
Boistelle, R. & Astier, J.-P. (1988). *J. Cryst. Growth*, **90**, 14–30.
Bon, C., Lehmann, M. S. & Wilkinson, C. (1999). *Acta Cryst.* D**55**, 978–987.
Bonneté, F., Madern, D. & Zaccaï, G. (1994). *J. Mol. Biol.* **244**, 436–447.
Budayova, M. (1998). Thesis. University Mediterranée, Marseille, France.
Budayova-Spano, M., Bonneté, F., Ferté, N., El Hajji, M., Meilleur, F., Blakeley, M. & Castro, B. (2006). *Acta Cryst.* F**62**, 306–309.
Budayova-Spano, M., Fisher, S. Z., Dauvergne, M.-T., Agbandje-McKenna, M., Silverman, D. N., Myles, D. A. A. & McKenna, R. (2006). *Acta Cryst.* F**62**, 6–9.
Budayova-Spano, M., Lafont, S., Astier, J.-P., Ebel, C. & Veesler, S. (2000). *J. Cryst. Growth*, **217**, 311–319.
Cacioppo, E., Munson, S. & Pusey, V. J. (1991). *J. Cryst. Growth*, **110**, 66–71.
Chayen, N. E. & Saridakis, E. (2002). *Acta Cryst.* D**58**, 921–927.
Chayen, N. E., Shaw Stewart, P. D., Maeder, D. L. & Blow, D. M. (1990) *J. Appl. Cryst.* **23**, 297–302.
Chernov, A. A. (2003). *J. Struct. Biol.* **142**, 3–21.
Christopher, G. K., Phipps, A. G. & Gray, R. J. (1998). *J. Cryst. Growth*, **191**, 820–826.
Cipriani, F., Castagna, J., Wilkinson, C., Oleinek, P. & Lehmann, M. (1996). *J. Neutron Res.* **4**, 79–85.
Coates, L., Erskine, P. T., Wood, S. P., Myles, D. A. A. & Cooper, J. B. (2001). *Biochemistry*, **40**, 13149–13157.
Ducruix, A. & Giegé, R. (1992). *Crystallization of Nucleic Acids and Proteins. A Practical Approach*, pp. 73–98. Oxford University Press.
Ducruix, A. F. & Riès-Kautt, M. M. (1990). *Methods*, **1**, 25–30.
Fisher, S., Maupin, C., Budayova-Spano, M., Govindasamy, L., Tu, C., Agbandje-McKenna, M., Silverman, D., Voth, G. & McKenna, R. (2007). In the press.
Gamble, T. R., Clauser, K. R. & Kossiakoff, A. A. (1994). *Biophys. Chem.* **53**, 15–25.
Garavito, R. M. & Picot, D. (1991). *J. Cryst. Growth*, **110**, 89–95.
Garcia-Ruiz, J. M. (2003). *J. Struct. Biol.* **142**, 22–31.
Gripon, C., Legrand, L., Rosenman, O., Vidal, O., Robert, M. C. & Boue, F. (1997). *J. Cryst. Growth*, **177**, 238–247.
Haire, L. F. & Blow, D. M. (2001). *J. Cryst. Growth*, **232**, 17–20.
Hazemann, I., Dauvergne, M. T., Blakeley, M. P., Meilleur, F., Haertlein, M., Van Dorsselaer, A., Mitschler, A., Myles, D. A. & Podjarny, A. (2005). *Acta Cryst.* D**61**, 1413–1417.
Kresheck, G. C., Schneider, H. & Scheraga, H. A. (1965). *J. Phys. Chem.* **69**, 3132–3144.
Lorber, B. & Giegé, R. (1992). *J. Cryst. Growth*, **122**, 168–175.
Luft, J. R. & DeTitta, G. (1997). *Methods Enzymol.* **276**, 110–131.
Lumry, R., Smith, E. L. & Glantz, R. R. (1951). *J. Am. Chem. Soc.* **73**, 4330–4340.
McPherson, A., Kuznetsov, Y. G., Malkin, A. & Plomp, M. (2003). *J. Struct. Biol.* **142**, 32–46.
Maeda, M., Chatake, T., Tanaka, A., Ostermann, A. & Niimura, N. (2004). *J. Synchrotron Rad.* **11**, 41–44.
Mitchell, E., Houles, C., Sudakevitz, D., Wimmerova, M., Gautier, C., Perez, S., Wu, A. M., Gilboa-Garber, N. & Imberty, A. (2002). *Nature Struct. Biol.* **9**, 918–921.
Myles, D. A. A., Bon, C., Langan, P., Cipriani, F., Castagna, J. C. & Wilkinson, C. (1998). *Physica B*, **241–243**, 1122–1130.
Ng, J. D., Lorber, B., Witz, J., Theobald-Dietrich, A., Kern, D. & Giegé, R. (1996). *J. Cryst. Growth*, **168**, 50–62.
Niimura, N., Arai, S., Kurihara, K., Chatake, T., Tanaka, I. & Bau, R. (2006). *Cell. Mol. Life Sci.* **63**, 285–300.
Rosenberger, F., Howard, S. B., Sowers, J. W. & Nyce, T. A. (1993). *J. Cryst. Growth*, **129**, 1–12.
Sazaki, G., Kurihara, K., Nakada, T., Miyashita, S. & Komatsu, H. (1996). *J. Cryst. Growth*, **169**, 355–360.
Sennoga, C., Heron, A., Seddon, J. M., Templer, R. H. & Hankamer, B. (2003). *Acta Cryst.* D**59**, 239–246.
Shu, F., Ramakrishnan, V. & Schoenborn, B. P. (2000). *Proc. Natl Acad. Sci. USA*, **97**, 3872–3877.
Tuominen, V. U., Myles, D. A. A., Dauvergne, M.-T., Lahti, R., Heikinheimo, P. & Goldman, A. (2004). *Acta Cryst.* D**60**, 606–609.
Veesler, S., Puel, F. & Fevotte, G. (2003). *STP Pharma Prat.* **13**, 1–32.